



A binary trait model reveals the fitness effects of HIV-1 escape from T cell responses

Yirui Gao^a and John P. Barton^{a,b,c,1}

Edited by James Bull, University of Idaho, Moscow, ID; received March 14, 2024; accepted January 15, 2025

Natural selection often acts on multiple traits simultaneously. For example, the virus HIV-1 faces pressure to evade host immunity while also preserving replicative fitness. While past work has studied selection during HIV-1 evolution, as in other examples where selection acts on multiple traits, it is challenging to quantitatively separate different contributions to fitness. This task is made more difficult because a single mutation can affect both immune escape and replication. Here, we develop an evolutionary model that disentangles the effects of escaping CD8⁺ T cell-mediated immunity, which we model as a binary trait, from other contributions to fitness. After validation in simulations, we applied this model to study within-host HIV-1 evolution in a clinical dataset. We observed strong selection for immune escape, sometimes greatly exceeding past estimates, especially early in infection. Conservative estimates suggest that roughly half of HIV-1 fitness gains during the first months to years of infection can be attributed to T cell escape. Our approach is not limited to HIV-1 or viruses and could be adapted to study the evolution of quantitative traits in other contexts.

evolution | quantitative traits | HIV | statistical inference

Natural selection acts on phenotypic traits, as individuals with traits that are well adapted to their environment enjoy relative reproductive success. Understanding how selective pressures shape evolution is a major goal of evolutionary biology. Applications include studying the drug resistance in bacteria (1) and patterns of evolution in cancer (2) or viruses (3).

In population genetics, methods have been developed to detect natural selection by examining the genetic diversity of a population and how it changes over time (4–11). However, inferred selection for a particular allele is not always easy to interpret. A single mutation can affect multiple traits, each of which may be subject to selection. Many phenotypic traits are also polygenic, meaning that they are affected by genetic variation at multiple sites and/or genes (12, 13). How can selection for a particular trait be disentangled from other evolutionary forces?

To approach this question, we developed a model to quantify selection on a binary trait, distinct from other contributions to fitness, using sequence data from an evolving population. Our model is motivated in particular by HIV-1 infection. HIV-1 evolves rapidly during infection, and specific mutations allow the virus to escape immune control (14–17). Past work has shown that the pressure to escape from CD8⁺ T cell responses is particularly strong (11, 18–20), though this is difficult to quantify precisely (20–22). While CD8⁺ T cell escape mutations can rapidly sweep through viral populations, the same mutations also often revert when the virus is transmitted to a new individual with a different immune response (18, 20, 23–25). This suggests that some escape mutations may harm viral replication in the absence of immune pressure.

After testing our approach in simulations, we applied it to study viral evolution in a dataset derived from 13 people living with HIV-1 (PLHIV). In these data, we observed strong selection for CD8⁺ T cell escape independent of other contributions to fitness. This was balanced by a decrease in the estimated fitness effects of specific escape mutations, compared to estimates in a model without the escape trait. Remarkably, we found that fitness gains due to CD8⁺ T cell escape were responsible for roughly half of the gains in viral fitness estimated from data, especially early in infection. Reversions to clade consensus were also strongly selected, comprising roughly a quarter of viral fitness gains after several years of evolution. Thus, in this dataset, we found that the vast majority of HIV-1 adaptation was driven by CD8⁺ T cell escape and reversions.

While the current work focuses on HIV-1 evolution, our framework for estimating the strength of selection on a binary trait is generic. This approach could be applied to study trait evolution in other contexts using temporal sequence data.

Significance

In general, the fitness or reproductive success of an organism depends on multiple traits. However, determining the fitness contributions of different traits from data is challenging. Here, we used a binary trait model to disentangle the fitness effects of HIV-1's evasion of CD8⁺ T cells from other contributions to viral replication. Analysis of clinical data suggests that HIV-1 evolution is best described by models with strong selection for T cell escape, but where individual escape mutations may impose a modest cost on HIV-1 replication. Our findings underscore the role of immune escape in the evolutionary dynamics of HIV-1. The trait model we develop could also be applied more generally beyond HIV-1.

Author affiliations: ^aDepartment of Physics and Astronomy, University of California, Riverside, CA 92521; ^bDepartment of Computational and Systems Biology, University of Pittsburgh School of Medicine, Pittsburgh, PA 15213; and ^cDepartment of Physics and Astronomy, University of Pittsburgh, Pittsburgh, PA 15213

Author contributions: Y.G. and J.P.B. designed research; performed research; contributed new reagents/analytic tools; analyzed data; and wrote the paper.

The authors declare no competing interest.

This article is a PNAS Direct Submission.

Copyright © 2025 the Author(s). Published by PNAS. This article is distributed under Creative Commons Attribution-NonCommercial-NoDerivatives License 4.0 (CC BY-NC-ND).

¹To whom correspondence may be addressed. Email: jpbarton@pitt.edu.

This article contains supporting information online at <https://www.pnas.org/lookup/suppl/doi:10.1073/pnas.2405379122/-/DCSupplemental>.

Published February 19, 2025.

Results

CD8⁺ T Cell Escape As a Binary Trait. T cells are a vital part of the adaptive immune system. A subset of T cells that express CD8 on the cell surface specializes in eliminating intracellular pathogens and cancer. Each T cell is equipped with a T cell receptor (TCR) that binds to a specific peptide, roughly 10 amino acids in length, which can be displayed by major histocompatibility complex type I (MHC-I) molecules on the target cell surface. When an activated CD8⁺ T cell binds to its cognate antigen, this can trigger the release of cytotoxins that kill the target cell. CD8⁺ T cells that recognize peptides derived from viral proteins can thus play an important role in controlling infection by killing infected cells before they have the chance to release viral particles. The importance of cytotoxic T cells in the context of HIV-1 infection has been appreciated since the early days of HIV-1 research (26).

Here, we model the susceptibility of HIV-1 viruses to killing by CD8⁺ T cell clones as a binary trait. That is, for each HIV-1-specific T cell clone within an individual, each virus is either vulnerable (0) or not (1). This is determined by whether or not viral proteins contain the peptide that a T cell binds, which is also referred to as an epitope.

In principle, one may imagine that states of partial immunity are possible: a virus may not express precisely the same epitope that a CD8⁺ T cell recognizes, but it may express one that is similar enough that it can also be detected by T cells. However, the binding of TCRs to peptide–MHC-I complexes is highly specific. While experiments have shown that some TCRs are cross-reactive to highly similar peptides, most mutations within the epitope abrogate T cell recognition (27–30). Thus, as we describe below, we modeled HIV-1 susceptibility to CD8⁺ T cells as “all or nothing,” where any nonsynonymous mutation within a T cell epitope results in a loss of immune recognition. We note that the binary state of immune escape is determined separately for each epitope, such that a particular virus may bear mutations that allow it to escape recognition from one CD8⁺ T cell clone while remaining sensitive to others.

Evolutionary Model Including Selection on Binary Traits. Our starting point is a Wright–Fisher model, which describes the evolution of a population of N individuals represented by genetic sequences of length L . For simplicity, in the main text, we will assume that genetic variants are binary, with each locus consisting of either a wild-type or mutant allele (see *SI Appendix* for a more detailed model). During each generation of replication, the probability that an individual replicates is proportional to its fitness. We write the fitness f_a of an individual with sequence a as

$$f_a = 1 + \sum_i^L s_i g_i^a + \sum_n^\Lambda s_n g_n^a. \quad [1]$$

Here, the s_i are selection coefficients that quantify the fitness effects of the mutant allele at each site i . The g_i^a are indicator variables, with g_i^a equal to one if sequence a has a mutant allele at site i , and zero otherwise. The last terms in Eq. 1 give the fitness contributions of the binary traits (CD8⁺ T cell escape, in our case; see Fig. 1E for an example). The n index labels different CD8⁺ T cell epitopes, with s_n quantifying the fitness effect of escape for the epitope labeled n . Unlike a regular locus, the binary trait can be seen as a “virtual” locus. Since multiple mutations within an epitope can confer escape, determining g_n^a requires considering genetic variation at multiple loci. We set g_n^a to one

if sequence a contains one or more nonsynonymous mutations within epitope n , and zero otherwise. This definition ensures that a single mutation is sufficient to confer immune escape for a particular epitope and that additional mutations within the same epitope do not further enhance escape effects. Although the effect of multiple mutations within a single epitope on escape is not cumulative, the escape effects from mutations in *different* epitopes add together (Fig. 1E). This model extends the simple additive fitness model used in a prior study of HIV-1 evolution, where the fitness benefits and costs of escape were effectively combined in the selection coefficients for escape mutations (11).

In addition to natural selection, our model includes spontaneous mutations, recombination, and genetic drift. We assume a simple probability μ per site per generation for the allele at each site i to change from wild-type (WT) to mutant (and vice versa). This can easily be extended to model different, asymmetric mutation rates between nucleotides in a realistic sequence model (*SI Appendix*). Genetic drift due to the finite population size of N individuals adds randomness to the evolutionary dynamics.

For HIV-1, recombination can occur when two different viruses coinfect the same cell and RNA from each of them is packaged in new virions. When virions containing distinct RNAs infect new cells, the reverse transcriptase can switch between RNA templates, producing recombinant DNA. The two components of this process are the coinfection rate, p_c , and the template switching rate, p_s . Estimates of the effective recombination rate $r \sim p_c p_s$ are high, with $r = 1.4 \times 10^{-5}$ (31). This is comparable to estimates of HIV-1 mutation rates (32). Following recent work showing that HIV-1 recombination occurs more frequently in PLHIV with higher viral loads as the probability that multiple viruses coinfect the same cell increases with viral load (33), we allowed the overall recombination rate to vary over time along with the measured viral load within each individual (*SI Appendix*).

Inference of Natural Selection from Temporal Genetic Data.

We developed a statistical inference method to infer selection, including both selection coefficients s_i for individual mutations and coefficients s_n for binary traits, from sequence data sampled over time. We assume that the mutations that affect the binary trait(s) are known; alternative approaches would be required to infer which mutations contribute to a trait. Our approach works by computing the probabilities of different evolutionary histories (i.e., frequencies of individual sequences in the population over time) as a function of the selection coefficients. We then find the selection coefficients that maximize the posterior probability of the data using Bayes’ theorem.

To make this inference problem tractable, we used a number of approximations and analytical techniques. First, we considered our evolutionary model in the so-called diffusion limit (34). In this limit, we assume that the population size N is very large, and that the selection coefficients s_i , trait coefficients s_n , mutation probabilities μ , and recombination probability r are small. We can then derive effective equations for the dynamics of the allele frequencies x_i and the trait frequencies x_n , which are described by a Fokker–Planck equation (*SI Appendix*). Allele frequencies x_i are defined as the fraction of individuals in the population with a mutant allele at site i , and trait frequencies x_n represent the fraction of individuals with a mutant allele at least one of the epitope sites for epitope n .

While the effective equations are mathematically complicated, their meaning can be clearly interpreted. Natural selection, mutation, and recombination drive deterministic changes in allele and/or trait frequencies, while the finite population size

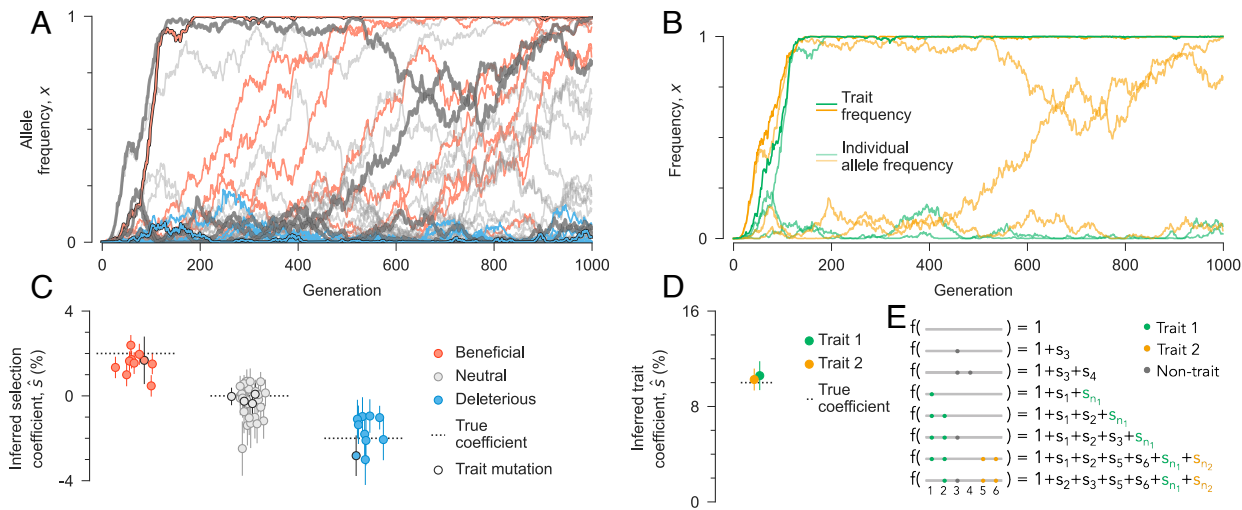


Fig. 1. Recovering selection on individual mutations and traits from temporal genetic data. (A) Simulated mutant allele frequency trajectories. Outlined allele frequencies represent the alleles that affect one of the two traits. (B) Trait frequencies and their contributing individual mutant allele frequencies (outlined in A) in the same simulation. Trait frequencies can approach one even when the frequencies of contributing alleles remain modest. The fitness contributions of individual mutations (C) and traits (D) that we infer are close to their true values. In (C) error bars with bold outlines represent alleles that affect the traits. (E) Illustration of the fitness function (Eq. 1). As an example, we consider a simple sequence with 6 sites and 2 binary traits whose values are determined by the first and last pair of sites in the sequence. Mutations within those trait sites (i.e., CD8⁺ T cell epitopes in the context of HIV-1) affect fitness in two ways: through the intrinsic fitness effect of the mutation, s_i , and through the fitness effect of the trait, s_n . Here, we show several examples of the net fitness effects of multiple mutations at different sites. Simulation parameters: $L = 50$ loci with two alleles at each locus (mutant and WT), ten beneficial mutants with $s = 0.02$, 30 neutral mutants with $s = 0$ and ten deleterious mutants with $s = -0.02$. We consider two binary traits, each with three contributing alleles and trait coefficients $s = 0.1$. Mutation probability per site per generation $\mu = 2 \times 10^{-4}$, recombination probability per site per generation $r = 2 \times 10^{-4}$, population size $N = 10^3$. The initial population contains all WT sequences, evolved over $T = 1,000$ generations.

contributes to noise. Alleles and traits are likely to increase in frequency if they appear on sequences that have higher fitness than the average fitness of the population. Mutation introduces new genetic variation, driving allele and trait frequencies away from zero or one. The effects of recombination are more subtle, with no net effect on expected changes in allele frequencies. However, recombination can drive changes in trait frequencies in a way that depends on the arrangement of mutations within the epitope (SI Appendix).

Finally, we used methods from statistical physics to convert the Fokker–Planck equation into a path integral (11, 35–38) (SI Appendix). The path integral quantifies the likelihood of different evolutionary histories or “paths” as a function of the selection coefficients. We can then derive an analytical expression for the vector of selection coefficients \hat{s} , including both the s_i and the s_n , that best fits the data (SI Appendix),

$$\hat{s} = (C_{\text{int}} + \gamma I)^{-1} (\Delta \mathbf{x} - \boldsymbol{\mu}_{\text{fl}} - \mathbf{R}_{\text{fl}}). \quad [2]$$

Here, C_{int} is the allele/trait frequency covariance matrix integrated over time, which accounts for the speed of evolution and the correlations between mutations/traits. The parameter γ specifies the width of a Gaussian prior distribution for the selection coefficients, and I is the identity matrix. The net change in allele/trait frequencies over the trajectory is $\Delta \mathbf{x}$. Finally, $\boldsymbol{\mu}_{\text{fl}}$ and \mathbf{R}_{fl} quantify the expected cumulative change (or flux) in allele/trait frequencies due to mutation and recombination, respectively. Intuitively, Eq. 2 attributes net changes in allele/trait frequencies that are not already explained by mutation or recombination to natural selection. The speed of evolution and the genetic background then control how beneficial or deleterious an allele or trait is inferred to be.

Performance on Simulated Data. To benchmark the performance of our method, we simulated population evolution in

the Wright–Fisher model using the fitness function defined in Eq. 1 (Fig. 1). We considered sequences with $L = 50$ loci (10 beneficial with selection coefficients $s = 2\%$, 30 neutral, and 10 deleterious with selection coefficients $s = -2\%$), with a population size of $N = 1,000$ individuals. We also included strong selection ($s = 10\%$) on $\Lambda = 2$ binary traits, each with three contributing alleles that were randomly chosen across the sequence. Individuals thus receive a substantial increase in fitness for mutations in at least one of the trait sites, but multiple mutations confer no additional benefit. Fig. 1 shows that our method is able to distinguish between beneficial, neutral, and deleterious alleles, and to estimate selection on these binary traits. When selection varies over time, the constant coefficients that we infer are typically similar to time-averaged ones (11) (SI Appendix, Fig. S1).

Robustness to Limited Sampling. Real datasets often face significant limitations in both the number of sequences that can be obtained and the frequency of sampling. To test the robustness of our approach to finite sampling, we ran 100 simulations across a wide range of sampling conditions. We assessed our ability to accurately identify selection by computing the average area under the receiver operating characteristic for classifying beneficial/deleterious mutations. We also computed the normalized root mean square error for the inferred trait coefficients. While inference becomes more difficult with limited sampling, declines in performance occur gradually (SI Appendix, Fig. S2). Our method is particularly robust to limited numbers of sequences, with the ability to identify beneficial or deleterious mutations using as little as 10 sequences per time point.

Identifiability of Trait Coefficients. As shown in Eq. 1, mutations at sites that affect binary traits can contribute two terms to fitness: a selection coefficient s_i for the individual (i th) mutation and the trait coefficient s_n . Thus, it is natural to ask what conditions are

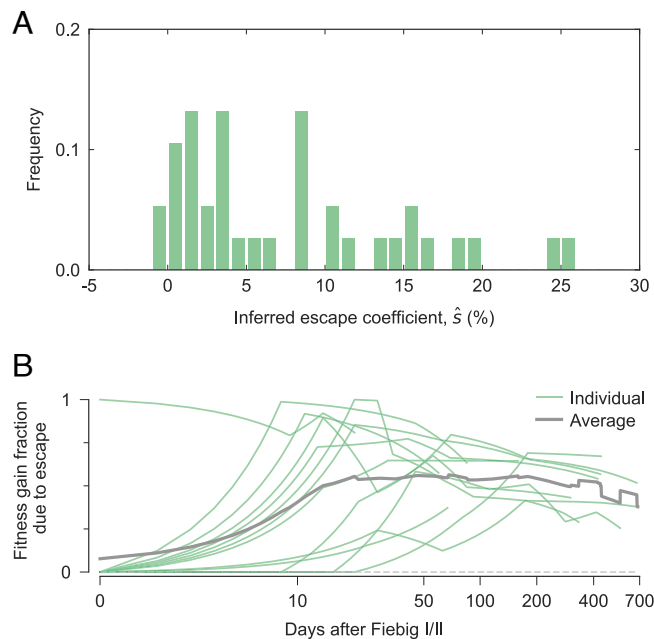


Fig. 2. CD8⁺ T cell escape is strongly selected and contributes substantially to intrahost HIV-1 fitness gains. (A) Distribution of inferred fitness effects of CD8⁺ T cell escape in HIV-1 data. Mutations within T cell epitopes allow infected cells to escape killing by T cells, thus allowing the virus to continue productive replication. (B) The fraction of the total increase in within-host HIV-1 fitness inferred for each of the 13 PLHIV that is due to CD8⁺ T cell escape.

necessary for the trait coefficient to be statistically identifiable, independent from the selection coefficients. Mathematically, the selection and trait coefficients are obtained by solving a linear equation, Eq. 2, which has the form $Ax = b$. Here, the matrix $A = C_{\text{int}} + \gamma I$ and x is the vector of selection and trait coefficients, \hat{s} . We can then assess which of the parameters (selection and trait coefficients) are linearly independent by computing the reduced row echelon form of A , which means that they are independently identifiable (36). To focus on the statistics of the data alone, we exclude the regularization term γI in this analysis, as this factor renders all parameters trivially linearly independent.

Intuitively, the trait coefficient will be linearly dependent if the trait is totally correlated (i.e., always observed together) with any other mutation. This means that at least two trait-associated mutations must be observed to independently estimate the corresponding trait coefficient s_{η} . In addition, both single mutants and a double mutant, which bears two mutations that affect the trait, must be present in the data.

Selection for Immune Escape in Intra-host HIV-1 Evolution. We applied our approach to study HIV-1 evolution using sequence data from 13 PLHIV (39) (SI Appendix). For each individual, longitudinal HIV-1 half-genome sequences were collected from around the time of peak viral load up to several months or years afterward. This time spans both the acute and chronic phases of infection. Early-phase CD8⁺ T cell epitopes were also carefully verified (30, 39), which allowed us to identify putative CD8⁺ T cell escape mutations. We then estimated the selection coefficients for individual HIV-1 mutations and T cell escape across all 13 PLHIV. Donors did not receive antiretroviral drug treatment during this study.

In order to confidently separate the fitness contribution of escape as a trait from the individual escape mutations, we focused on a well-sampled subset of all T cell epitopes. Specifically, we included only escape coefficients (i.e., trait coefficients T cell escape) whose parameters were statistically identifiable in this dataset following the procedure defined in the previous section (36). Out of 71 CD8⁺ T cell epitopes in this dataset containing at least one nonsynonymous mutation, 37 escape coefficients can be estimated independently from the fitness effects of individual mutations. For the remaining 34 epitopes, we still estimated selection coefficients for individual escape mutations, but we did not attempt to disentangle the contributions of T cell escape versus intrinsic fitness.

Overall, we found very strong selection for CD8⁺ T cell escape in most epitopes (Fig. 2A). Inferred escape coefficients ranged from nearly neutral to highly beneficial ($s \sim 26\%$), with a mean value of 8%. Fig. 3 shows a typical example of HIV-1 evolution to escape from T cell responses across two epitopes in individual CH470. Here, multiple escape mutations are observed for each epitope, making it challenging to infer the strength of selection for escape by looking at single mutations alone.

Next, we quantified how much CD8⁺ T cell escape contributes to observed changes in HIV-1 fitness *in vivo*. To do this, we computed the fitness of each sequence in each individual and measured the fraction of fitness increase (relative to the transmitted/founder (TF) virus) due to escape coefficients. Here, we also included the contribution from escape mutations in epitopes where escape coefficients were not separately estimated. We observed a consistent pattern where escape mutations were rapidly selected within the first weeks of infection, followed by a long, slow decline (Fig. 2B). In only 10 d, T cell escape comprises roughly half of HIV-1 fitness gains. This is especially remarkable given that the identified T cell epitopes cover less than 2% of the HIV-1 proteome in these individuals.

Reversions and the Intrinsic Fitness Effects of CD8⁺ T Cell Escape Mutations. CD8⁺ T cell escape mutations have been observed to revert after the virus is transmitted to a new host (18, 20, 23–25), suggesting that escape mutations may be deleterious in the absence of immune pressure. Before explicitly modeling T cell escape as a trait, a large fraction (37%) of escape mutations are inferred to be substantially beneficial ($\hat{s} > 1\%$; SI Appendix, Fig. S3). When escape coefficients are included, the distribution of inferred selection coefficients for escape mutations shifts substantially toward more deleterious values, with a peak

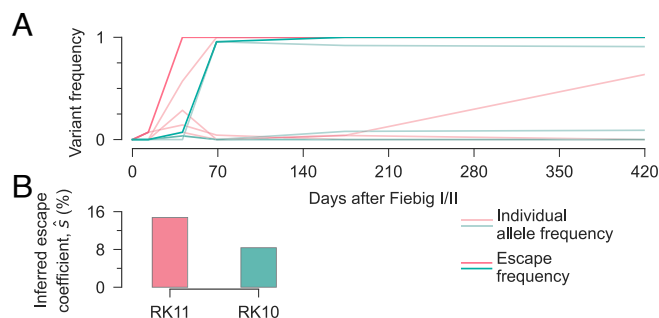


Fig. 3. Estimates of selection for CD8⁺ T cell escape in a simple example. (A) Frequency of individual escape mutations and the escape trait for two epitopes in the 3' half-genome for individual CH470. Escape in each epitope is mediated by multiple mutations. (B) We infer strong positive selection for escape for all two epitopes.

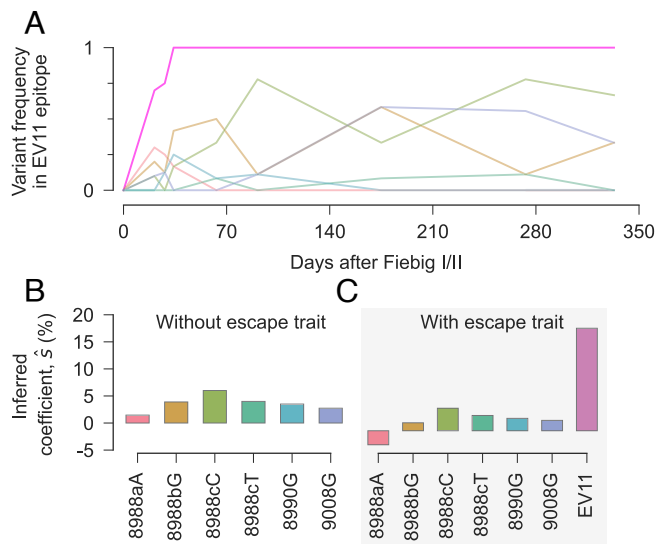


Fig. 4. Inclusion of escape as a trait increases the inferred selective advantage of escape and decreases the apparent advantage of individual escape mutations. (A) Allele frequencies and escape frequency for epitope EV11 in individual CH131. Escape at this epitope is complex, with contributions from six distinct mutations. (B) Without treating escape as a trait, all EV11 escape mutations are inferred to be positively selected. (C) When the selective advantage of escape is considered separately, the inferred selection coefficients for individual mutations become more deleterious. Conversely, the estimated advantage of EV11 escape is substantial, much larger than the inferred selection coefficient for any individual escape mutation without the escape trait.

near zero. In this case, only 16% of escape mutations are inferred to be substantially beneficial. HIV-1 evolutionary dynamics within each host are therefore best explained by a model where CD8⁺ T cell escape provides a substantial fitness benefit, which is achieved through escape mutations that may be nearly neutral or even moderately deleterious.

Fig. 4 shows an example of the shift in inferred selection coefficients for escape mutations after escape is modeled as a trait. Escape at the EV11 epitope targeted by individual CH131 occurs rapidly. However, there is no single, primary escape mutation. Instead, a set of six escape mutations compete for dominance in the viral population. Without the inclusion of an escape coefficient, the inferred selection coefficients for all of these mutations are positive, with a maximum of around 6%. When we estimate an escape coefficient for EV11, the inferred selection coefficients for individual escape mutations shift to appear more deleterious. In addition, the inferred fitness benefit of escape for the EV11 epitope is around 15%, far higher than the selection coefficient for any individual escape mutation that we estimated in the absence of the escape coefficient.

The intrinsic fitness cost of escape mutations is also highlighted by the benefit of reversions toward the clade consensus sequence. Similar to our previous analysis for CD8⁺ T cell escape mutations, we computed the fraction of HIV-1 fitness gains in each individual that can be attributed to reversions over time. We observed that reversions contributed substantially to HIV-1 fitness in vivo, in a way that grows steadily over time (SI Appendix, Fig. S4). After several years of infection, an average of around 25% of HIV-1 fitness gains relative to the TF virus are due to reversions.

For both T cell escape and reversions, we note that fitness contributions are heterogeneously distributed across individual mutations. Inferred selection coefficients for both types of

mutations have long tails (SI Appendix, Fig. S5). A few, large selection coefficients thus make large contributions to fitness.

Stability of Inferred Selection Outside T Cell Epitopes. Changing the fitness model that we use to describe HIV-1 evolution can affect the fitness effects of mutations that we infer. For mutations within CD8⁺ T cell epitopes, these effects can be quite large, as described above (SI Appendix, Fig. S3). Does the inclusion of escape coefficients also affect mutations outside of T cell epitopes? Large changes in these selection coefficients could indicate that the inference process is highly sensitive to specific modeling choices, casting doubt on its reliability.

Overall, the inclusion of escape coefficients shifts the inferred effects of escape mutations, which are typically inferred to be highly beneficial without considering the escape trait, toward much more deleterious values, but without substantially reshaping the overall distribution of selection coefficients (SI Appendix, Fig. S5). Fig. 5 shows a representative example, demonstrating that inferred selection coefficients for individual mutations with and without the inclusion of escape coefficients are very strongly correlated. Most selection coefficients that change significantly are located within CD8⁺ T cell epitopes, as expected. However, the selection coefficient for one non-epitope mutation, 974A, undergoes a substantial change ($\hat{s} \sim 3\%$ to around 2% before and after the inclusion of escape coefficients, respectively). We found that 974A was strongly linked with 3951C, an escape mutation in the RL9 epitope, which potentially explains this difference.

In this example, we comprehensively explored the effects of linkage disequilibrium (i.e., correlations) between mutations/escape on inferred selection coefficients. Estimated selection coefficients for all mutations and traits are connected due to the integrated allele/trait frequency covariance matrix C_{int} in Eq. 2. For each escape mutation and trait j , we computed the selection coefficients that would be inferred if each other mutation/trait i was ignored, denoted \hat{s}_j^i (SI Appendix). The difference between the coefficient inferred for j using the full data and the coefficient inferred when mutation/trait i is held out yields the effect of linkage with i on j (11),

$$\Delta\hat{s}_{ij} = \hat{s}_j - \hat{s}_j^i. \quad [3]$$

Fig. 5C shows $\Delta\hat{s}_{ij}$ values for 974A, the escape coefficients for epitopes DL9, EK9, and RL9, and the individual escape mutations that occur within these epitopes. Here, we find that linkage disequilibrium with 3951C and RL9 escape mutants is indeed primarily responsible for the shift in selection inferred for 974A. The fitness benefit of escape partly explains the rise to fixation of 974A, reducing its estimated selection coefficient.

Discussion

In this paper, we developed a method to estimate the fitness effect of a binary trait, jointly with selection coefficients for individual mutations, from temporal genetic data. After validation in simulations, we applied this method to study intrahost HIV-1 evolution in a clinical dataset. We modeled CD8⁺ T cell escape as a binary trait to disentangle the contributions of immune evasion and intrinsic replication to HIV-1 fitness. In these data, HIV-1 evolution was best explained by models with strong selection for T cell escape, but with individual escape mutations that are typically nearly neutral. Reversions to clade consensus were also inferred to be beneficial. The contributions of reversions to HIV-1 fitness gains grew steadily over time.

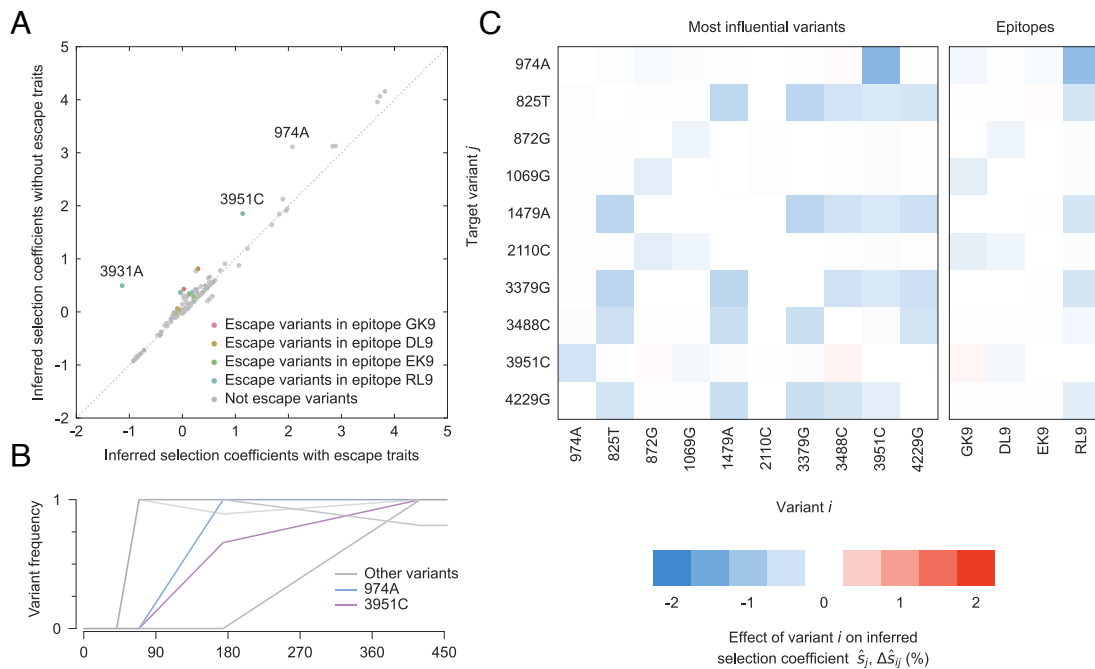


Fig. 5. Inclusion of escape as a trait only strongly affects inferred selection coefficients for escape mutations and alleles that are strongly linked to them. (A) Inferred selection coefficients with and without escape terms inferred from 5' HIV-1 half-genomes from individual CH470. There are three alleles with substantial shifts in inferred selection. Two of these (3931A and 3951C) are escape variants in RL9. (B) Allele frequencies for variants that appear frequently with 974A, demonstrating strong linkage with 3951C. (C) Linkage effects on inferred selection coefficients for mutations linked to 974A, and escape coefficients for the three CD8⁺ T cell epitopes. Effects show the strong interaction between variant 974A and variant 3951C, with RL9 escape decreasing the inferred selection coefficient for 974A.

Our findings are consistent with past observations that have reported strong selection for T cell escape (11, 18, 20, 39–41). However, here we found an even stronger benefit for CD8⁺ T cell escape compared to past work (11). There are also reasons to believe that the selection for T cell escape may be even stronger than what we have estimated. The Bayesian regularization that we have used controls the inference of large selection coefficients that are not well-supported by data, but it favors spreading the effects of a single large parameter (e.g., a large escape coefficient) into multiple smaller ones (e.g., selection coefficients for individual escape mutations) to maximize the posterior distribution. This is a well-known effect of L_2 -norm regularization. This effect could be alleviated in future work through the choice of a different prior distribution, though this could make the analytical derivation of the estimator for selection/trait coefficients more challenging.

The apparent selective advantage of reversions has also been noted in prior work (11, 20, 25). However, to our knowledge, the relative genome-wide contributions of immune escape across CD8⁺ T cell epitopes and reversions to HIV-1 fitness, and how these contributions vary over the first few years of infection, have not previously been quantified. Remarkably, after several years of infection, roughly three-quarters of within-host HIV-1 fitness gains can be attributed to CD8⁺ T cell escape or reversions (*SI Appendix, Fig. S6*). As discussed by Zanini and collaborators (20), the apparent consistency of selective pressures on HIV-1 across many PLHIV, reflected by strong selection for reversions, could help to explain the success of HIV-1 fitness models that are based on sequence conservation across hosts (30, 42–44).

Several previous studies have attempted to separately quantify the fitness benefits and costs of T cell escape and escape mutations, respectively, in HIV-1 or SIV (refs. 40, 41, 45, and 46). In contrast with the present work, these studies fit escape benefits and fitness costs by comparing two populations of individuals:

one in which a particular T cell epitope is targeted, and another (often HLA-mismatched) one that does not respond in the same way. Estimates of the fitness effects of escape vary. Some studies found very strong effects for particular epitopes (40, 41), whereas others estimated both escape benefits and costs that are very close to zero (46). Compared to these studies, the typical fitness benefit of escape that we observe is more moderate, with a median selection coefficient of around 4% (similar to ref. 45). However, as shown in Fig. 2, the fitness benefit of escape for some epitopes is inferred to be as high as 25%. Our results are most different from those of ref. 46, which may be partly attributable to differences in datasets. In the dataset that we use, viral sequences were obtained frequently, especially early in infection, and donors were not using antiretroviral drugs. For ref. 46, the shortest time between longitudinal samples was around 6 mo, and many individuals received some drug treatment. Our work also accounts for interference between viral variants, which can lead to much larger estimates of the fitness effects of beneficial mutations (11). While the inferred fitness effects of mutations for genetically similar viruses can be remarkably well-correlated across different hosts (47), some differences between our results and prior studies may also be due to the joint estimates of fitness effects across multiple individuals in prior work.

Our study has some limitations due to the constraints on the data available. While our approach is very robust to limited numbers of sequences, long gaps in time between samples limit our ability to fully resolve evolutionary dynamics, leading to less accurate inferences (*SI Appendix, Fig. S2*). In T cell epitopes, when there are few observed escape mutations, it is also statistically challenging to distinguish between the fitness effects of individual mutations and the fitness benefit of escape. This is why we have not attempted to estimate escape coefficients for epitopes with only one or two escape mutations.

The fitness model that we have used could also be extended. Our present model does not account for epistasis, which is prevalent in nature. Because our model does not include epistatic interactions, our estimates of the fitness effects of escape may be conflated with or affected by other epistatic interactions between escape mutations. For example, for epitopes with two observed escape mutations, the inferred escape coefficient could incorporate epistatic interactions between these mutations that are unrelated to T cell escape. While the form of our model was motivated by the study of HIV-1 escape from CD8⁺ T cell responses, it could apply binary traits in other evolutionary contexts as well. In future work, we aim to extend this approach to estimate selection on more general quantitative traits and explicitly account for epistasis between trait-affecting mutations. Ultimately, the development of new methods to fit more realistic models to data will improve our quantitative understanding of evolution.

Future studies should also consider time-varying selection. In principle, we may expect to observe time-varying selection for T cell escape as immune responses rise and fall. With our current approach, the selection coefficients that we estimate are roughly equivalent to the average selection coefficient when selection changes in time (11, 37) (*SI Appendix, Fig. S1*). In epitopes that accumulate multiple escape mutations, however, the trait coefficients that we estimate may be more similar to the strength of selection that originally drove escape, at least in cases where the individual escape mutations are not strongly deleterious. This is because the rate for escape to “revert” can be

quite slow when most viruses possess multiple escape mutations, requiring more than one mutation or recombination event for all escape mutations to be removed. In this case, it could be difficult to accumulate evidence for weaker selection for escape because sequences without any escape mutations are only produced rarely. Future work should examine how selection for immune escape varies with time, and how this is associated with the corresponding strength of immune responses.

Materials and Methods

Mathematical derivations, simulation details, and information about the HIV-1 data and data processing are presented in *SI Appendix*. The first five sections provide details about our evolutionary model and the associated inference framework. *SI Appendix, section 6* extends the basic model to incorporate multiple alleles per locus and asymmetric mutation probabilities. *SI Appendix, section 7* describes the simulation setup, sampling analysis, and time-varying selection study. The final three sections focus on HIV-1 data analysis, encompassing data processing procedures, linkage calculations, and recombination effects.

Data, Materials, and Software Availability. Data and code used in our analysis is available in the GitHub repository (48). This repository also contains Jupyter notebooks that can be run to reproduce our figures and analysis.

ACKNOWLEDGMENTS. The work of Y.G. and J.P.B. reported in this publication was supported by the National Institute of General Medical Sciences of the NIH under Award Number R35GM138233.

- J. Davies, D. Davies, Origins and evolution of antibiotic resistance. *Microbiol. Mol. Biol. Rev.* **74**, 417–433 (2010).
- R. Vendramin, K. Litchfield, C. Swanton, Cancer evolution: Darwin and beyond. *EMBO J.* **40**, e108389 (2021).
- A. S. Lauring, Within-host viral diversity: A window into viral evolution. *Annu. Rev. Virol.* **7**, 63–81 (2020).
- C. J. Illingworth, V. Mustonen, Distinguishing driver and passenger mutations in an evolutionary history categorized by interference. *Genetics* **189**, 989–1000 (2011).
- A. F. Feder, S. Kryazhimskiy, J. B. Plotkin, Identifying signatures of selection in genetic time series. *Genetics* **196**, 509–522 (2014).
- M. Lacerda, C. Seoighe, Population genetics inference for longitudinally-sampled mutants under strong selection. *Genetics* **198**, 1237–1250 (2014).
- M. Foll, H. Shim, J. D. Jensen, WFABC: A wright-fisher ABC-based approach for inferring effective population sizes and selection coefficients from time-sampled data. *Mol. Ecol. Resour.* **15**, 87–98 (2015).
- J. Terhorst, C. Schlötterer, Y. S. Song, Multi-locus analysis of genomic time series data from experimental evolution. *PLoS Genet.* **11**, e1005069 (2015).
- J. G. Schraiber, S. N. Evans, M. Slatkin, Bayesian inference of natural selection from allele frequency time series. *Genetics* **203**, 493–511 (2016).
- T. Taus, A. Futschik, C. Schlötterer, Quantifying selection with pool-seq time series data. *Mol. Biol. Evol.* **34**, 3023–3034 (2017).
- M. S. Sohail, R. H. Louie, M. R. McKay, J. P. Barton, MPL resolves genetic linkage in fitness inference from complex evolutionary histories. *Nat. Biotechnol.* **39**, 472–479 (2021).
- J. K. Pritchard, J. K. Pickrell, G. Coop, The genetics of human adaptation: Hard sweeps, soft sweeps, and polygenic adaptation. *Curr. Biol.* **20**, R208–R215 (2010).
- N. Barghi, J. Hermisson, C. Schlötterer, Polygenic adaptation: A unifying framework to understand positive selection. *Nat. Rev. Genet.* **21**, 769–781 (2020).
- P. Borrow *et al.*, Antiviral pressure exerted by HIV-1-specific cytotoxic T lymphocytes (CTLs) during primary infection demonstrated by rapid selection of CTL escape virus. *Nat. Med.* **3**, 205–211 (1997).
- P. J. Goulder *et al.*, Late escape from an immunodominant cytotoxic T-lymphocyte response associated with progression to AIDS. *Nat. Med.* **3**, 212–217 (1997).
- A. D. Price *et al.*, Positive selection of HIV-1 cytotoxic T lymphocyte escape variants during primary infection. *Proc. Natl. Acad. Sci. U.S.A.* **94**, 1890–1895 (1997).
- A. J. McMichael, P. Borrow, G. D. Tomaras, N. Goonetilleke, B. F. Haynes, The immune response during acute HIV-1 infection: Clues for vaccine development. *Nat. Rev. Immunol.* **10**, 11–23 (2010).
- T. M. Allen *et al.*, Selective escape from CD8⁺ T-cell responses represents a major driving force of human immunodeficiency virus type 1 (HIV-1) sequence diversity and reveals constraints on HIV-1 evolution. *J. Virol.* **79**, 13239–13249 (2005).
- Y. Liu *et al.*, Selection on the human immunodeficiency virus type 1 proteome following primary infection. *J. Virol.* **80**, 9519–9529 (2006).
- F. Zanini *et al.*, Population genomics of inpatient HIV-1 evolution. *eLife* **4**, e11282 (2015).
- A. Schneidewind *et al.*, Transmission and long-term stability of compensated CD8 escape mutations. *J. Virol.* **83**, 3993–3997 (2009).
- K. A. Lythgoe, C. Fraser, New insights into the evolutionary rate of HIV-1 at the within-host and epidemiological levels. *Proc. R. Soc. B Biol. Sci.* **279**, 3367–3375 (2012).
- A. Leslie *et al.*, HIV evolution: CTL escape mutation and reversion after transmission. *Nat. Med.* **10**, 282–289 (2004).
- T. C. Friedrich *et al.*, Reversion of CTL escape-variant immunodeficiency viruses in vivo. *Nat. Med.* **10**, 275–281 (2004).
- B. Li *et al.*, Rapid reversion of sequence polymorphisms dominates early human immunodeficiency virus type 1 evolution. *J. Virol.* **81**, 193–201 (2007).
- B. Walker, A. McMichael, The T-cell response to HIV. *Cold Spring Harb. Perspect. Med.* **2**, a007054 (2012).
- J. K. Lee *et al.*, T cell cross-reactivity and conformational changes during TCR engagement. *J. Exp. Med.* **200**, 1455–1466 (2004).
- E. S. Huseby *et al.*, How the T cell repertoire becomes peptide and MHC specific. *Cell* **122**, 247–260 (2005).
- E. S. Huseby, F. Crawford, J. White, P. Marrack, J. W. Kappler, Interface-disrupting amino acids establish specificity between T cell receptors and complexes of major histocompatibility complex and peptide. *Nat. Immunol.* **7**, 1191–1199 (2006).
- J. P. Barton *et al.*, Relative rate and location of intra-host HIV evolution to evade cellular immunity are predictable. *Nat. Commun.* **7**, 11660 (2016).
- R. A. Neher, T. Leitner, Recombination rate and selection strength in HIV intra-patient evolution. *PLoS Comput. Biol.* **6**, e1000660 (2010).
- F. Zanini, V. Puller, J. Brodin, J. Albert, R. A. Neher, In vivo mutation rates and the landscape of fitness costs of HIV-1. *Virus Evol.* **3**, vey003 (2017).
- E. V. Romero, A. F. Feder, Elevated HIV viral load is associated with higher recombination rate in vivo. *Mol. Biol. Evol.* **41**, msad260 (2024).
- W. J. Ewens, *Mathematical Population Genetics: Theoretical Introduction* (Springer, 2004), vol. 27.
- V. Mustonen, M. Lässig, Fitness flux and ubiquity of adaptive evolution. *Proc. Natl. Acad. Sci. U.S.A.* **107**, 4248–4253 (2010).
- M. S. Sohail, R. H. Louie, Z. Hong, J. P. Barton, M. R. McKay, Inferring epistasis from genetic time-series data. *Mol. Biol. Evol.* **39**, msac199 (2022).
- B. Lee *et al.*, Inferring effects of mutations on SARS-CoV-2 transmission from genomic surveillance data. *Nat. Commun.* **16**, 441 (2025).
- K. Shimagaki, J. P. Barton, Bézier interpolation improves the inference of dynamical models from data. *Phys. Rev. E* **107**, 024116 (2023).
- M. K. Liu *et al.*, Vertical T cell immunodominance and epitope entropy determine HIV-1 escape. *J. Clin. Invest.* **123**, 380–393 (2012).
- C. S. Fernandez *et al.*, Rapid viral escape at an immunodominant simian-human immunodeficiency virus cytotoxic T-lymphocyte epitope exacts a dramatic fitness cost. *J. Virol.* **79**, 5721–5731 (2005).
- J. N. Mandl, R. R. Regoes, D. A. Garber, M. B. Feinberg, Estimating the effectiveness of simian immunodeficiency virus-specific CD8⁺ T cells from the dynamics of viral immune escape. *J. Virol.* **81**, 11982–11991 (2007).
- A. L. Ferguson *et al.*, Translating HIV sequences into quantitative fitness landscapes predicts viral vulnerabilities for rational immunogen design. *Immunity* **38**, 606–617 (2013).

43. J. K. Mann *et al.*, The fitness landscape of HIV-1 gag: Advanced modeling approaches and validation of model predictions by in vitro testing. *PLoS Comput. Biol.* **10**, e1003776 (2014).
44. R. H. Louie, K. J. Kaczorowski, J. P. Barton, A. K. Chakraborty, M. R. McKay, Fitness landscape of the human immunodeficiency virus envelope protein that is targeted by antibodies. *Proc. Natl. Acad. Sci. U.S.A.* **115**, E564–E573 (2018).
45. B. Asquith, C. T. T. Edwards, M. Lipsitch, A. R. McLean, Inefficient cytotoxic T lymphocyte-mediated killing of HIV-1-infected cells in vivo. *PLoS Biol.* **4**, e90 (2006).
46. H. R. Fryer *et al.*, Modelling the evolution and spread of HIV immune escape mutants. *PLoS Pathog.* **6**, e1001196 (2010).
47. K. S. Shimagaki, R. M. Lynch, J. P. Barton, Parallel HIV-1 evolutionary dynamics in humans and rhesus macaques who develop broadly neutralizing antibodies. bioRxiv [Preprint] (2024). <https://doi.org/10.1101/2024.07.12.603090> (Accessed 7 December 2024).
48. Y. Gao, J. P. Barton, Data from: "A binary trait model reveals the fitness effects of HIV-1 escape from T cell responses." GitHub. <https://github.com/bartonlab/paper-binary-trait-inference>. Deposited 4 March 2024.